Challenges in measuring spherical geometry using terrestrial laser scanners

Muralikrishnan, Balasubramanian; Rachakonda, Prem K.; Shilling, Katharine M.; Lee, Vincent D.; Sawyer, Daniel S.; Cheok, Geraldine S.; Cournoyer, Luc

Proceedings of the Annual Meeting of the ASPE 2017, 2017-11-01

CHALLENGES IN MEASURING SPHERICAL GEOMETRY USING TERRESTRIAL LASER SCANNERS

Bala Muralikrishnan[1], Prem Rachakonda[1], Meghan Shilling[1], Vincent Lee[1], Daniel Sawyer[1], Geraldine Cheok[1], and Luc Cournoyer[2]

[1]National Institute of Standards and Technology, Gaithersburg, MD 20899
[2]National Research Council of Canada, Ontario, Canada K1A0R6

INTRODUCTION

Terrestrial laser scanners (TLSs) measure 3D coordinates in a scene by recording the range, the azimuth angle, and elevation angle of discrete points on target surfaces. They are increasingly used in a variety of applications, including manufacturing and civil infrastructure systems. However, the error sources of these instruments are not yet adequately characterized. There is a lack of standardized test procedures [1] and detailed uncertainty budgets for TLS measurements are seldom available. As Lichti et al [2] described, measuring curved surfaces using TLS has always proved problematic. In this context, we describe here the challenges involved in measuring a spherical geometry using TLS.

Spherical geometry is commonly found in manufacturing environments. In addition, sphere targets are sometimes introduced into a scene to register scans from multiple positions of a TLS. Target spheres are also used to construct calibrated reference lengths to evaluate the performance of a TLS [3, 4]. A spherical geometry is preferred for registration and performance evaluation experiments because its geometry appears the same from all view points, and it is reasonably straightforward to reduce the point cloud data to a single point, its center.

However, from experiments performed at the laboratories of the Dimensional Metrology Group at NIST, we know that some TLS systems are incapable of obtaining a reliable point cloud from the surface of a spherical target. The changing surface curvature, averaging of the laser spot on the surface, multiple reflections from nearby surfaces and many other factors contribute to the scanned data of the sphere appearing either smaller (squished) or larger (flared) than the actual sphere. This not only means that the radius of the sphere is incorrectly determined but there is also an error in locating the center of the sphere, whose error direction depends on the scanner position. Center location error is of consequence in multiple applications including scan registration and scanner performance evaluation experiments conducted using scale bars with sphere targets on ends.

In this paper, we explore the problem of sphere measurements through experiments and simulations, highlighting the challenges in measuring as simple a geometry as a sphere using TLS.

SPHERE SQUISHING/FLARING AND UNCONSTRAINED RADIUS

Several factors affect the sphere point cloud data as mentioned earlier. We discuss experiments conducted to estimate the effect of mounting and point density on sphere radius in this section.

Effect of mounting

In order to examine the effect of mounting conditions on the observed sphere radius, we mounted a 50 mm nominal radius media-blasted aluminum semi-sphere in three different ways as shown in Fig. 1. In case (a), the sphere is mounted centrally on an 18 in × 18 in (45.72 cm x 45.72 cm) aluminum plate with a clearance of 0.5 in (1.27 cm) around the sphere. In case (b), laser absorbing black flock paper is glued around the sphere (forming a 1.5 in (3.81 cm) annulus) to absorb some of the secondary reflections. In case (c), the sphere is mounted on a much smaller aluminum plate that also has black flock paper glued on it.

The form error of the sphere was measured to be 10 µm on a coordinate measuring machine (CMM). The flatness of the plate (Fig. 1(a) and (b)) was measured on a CMM to be 55 µm over its entire surface but only 20 µm over a central circular region of radius 200 mm.

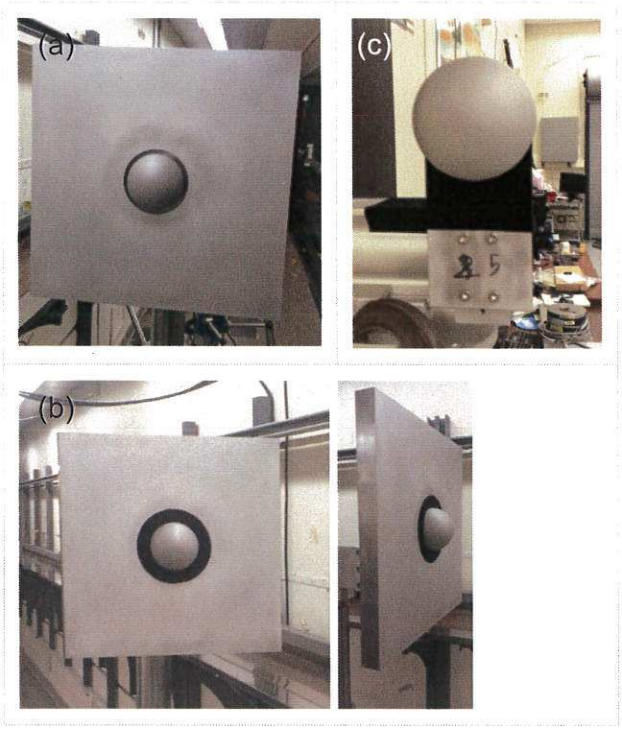

FIGURE 1. (a) a 50 mm radius sphere mounted centrally on an 18 in × 18 in (45.72 cm x 45.72 cm) plate, (b) 1.5 in (1.27 cm) ring of flock paper glued around the sphere to absorb secondary reflections, (c) sphere mounted on a smaller plate with flock paper glued on it

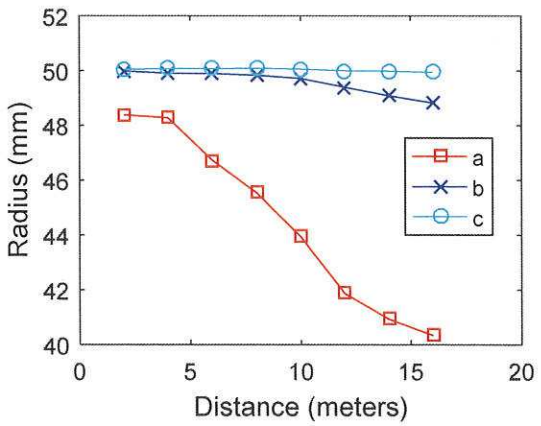

FIGURE 2. Unconstrained least-squares best-fit radius as a function of distance for three different cases of mounting, case (a) corresponds to Fig. 1(a), case (b) corresponds to Fig. 1(b), and case (c) corresponds to Fig. 1(c).

The sphere is scanned four times each at distances of 2 m through 16 m in steps of 2 m and an unconstrained least-squares best-fit sphere is fit to the data. The scans were performed at 90 points per degree (ppd) along the azimuth and elevation angle directions. Fig. 2 shows the unconstrained least-squares best-fit radius (average from the four scans) for each of the three cases which illustrates that the mounting of the sphere has a significant influence on the unconstrained radius.

When mounted on a plate with no laser absorbing flock paper, secondary reflections from the plate have a significant impact on the data quality causing the sphere to appear increasingly squished at far distances. The radius drops from 48 mm at 2 m down to as low as 40 mm at 16 m. In case (c) where a much smaller plate with laser absorbing flock paper is used, secondary reflections are significantly reduced resulting in the radius holding steady at 50 mm even at 16 m scan distance. It should be noted that points in the outer periphery of the sphere are not considered in the determination of the center; only the region of the sphere that lies within a central cone angle of 120° are used in the calculation.

Effect of point density

To examine the effect of point density on the observed radius, a white plastic sphere of nominal radius 75 mm is scanned at different point densities from six ppd through 57 ppd (equal sampling intervals along both the vertical and horizontal axis directions). The sphere was placed at a distance of about 5 m from the instrument. The data is fit using an unconstrained radius least-squares best-fit sphere algorithm and the resulting radius is shown in Fig. 3.

Changing point density affects the mirror rotation speed (for the instrument used in this study), likely resulting in changing the extent of spatial averaging over the curved sphere surface, thereby affecting sphere radius. Fig. 3 shows the radius changes by at least 3 mm from 6 ppd to 57 ppd.

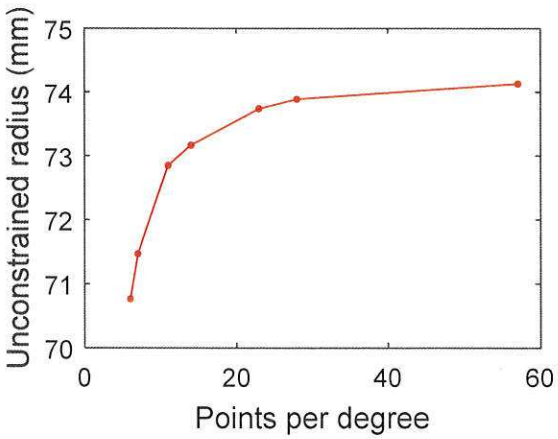

FIGURE 3. Unconstrained radius as a function of point density

SPHERE SQUISHING/FLARING AND CENTER ERROR

While the error in the radius can be determined by comparing the radius obtained by the TLS against that obtained using a reference instrument such as a coordinate measuring machine (CMM), the error in the center is not as easily estimated because the location of the true center of the sphere is an unknown quantity. As the amount of squishing and flaring increases, it proportionally changes the location of the center as determined by the TLS.

The error in the center location arises because the squishing/flaring effect is more pronounced on the outer periphery of the sphere, i.e., region where the angle of incidence is larger. It is assumed that the TLS records the correct range when the laser beam is normally incident on the surface, i.e., the region of the sphere that is closest to the TLS (see Fig. 4). A least-square fit, constrained to the calibrated radius of the sphere, does not eliminate the center error as described in the simulations in the next sub-section.

To estimate the magnitude of the error in the center location of the sphere, we consider the artifact shown in Fig. 1 (b). We refer to this as the plate-sphere artifact. The distance from the center of the sphere to the plate is calibrated using a CMM. The plate serves as the reference for the TLS measurements; an error in locating the center of the sphere will appear as an error in the sphere-center to plate distance. The idea, therefore, is to infer the sphere center location error from the error in the sphere-center to plate distance.

In the next sub-section, we describe a simulation to estimate the error in the center based on the extent of squishing/flaring, i.e., the unconstrained radius obtained from the measured point cloud. Subsequently, we describe experimental data in support of this simulation.

Simulations

The schematic in Fig. 4 illustrates profiles of a real sphere surface (solid gray line) and the point cloud (solid black line) of that sphere as measured by a TLS system. The measured surface in this illustration appears more ellipsoidal than spherical, with the long axis oriented along the ranging direction, i.e., the sphere appears squished. The data are segmented so that data within a cone opening angle of 120° is retained. As can be seen in the figure, a constrained fit based on the calibrated radius of the sphere produces a center O_1 that is farther away from the TLS than the true center O. An unconstrained fit produces a center O_2 that is closer to the TLS than the true center O.

To evaluate the effect of sphere squishing/flaring, the quantity of interest is the

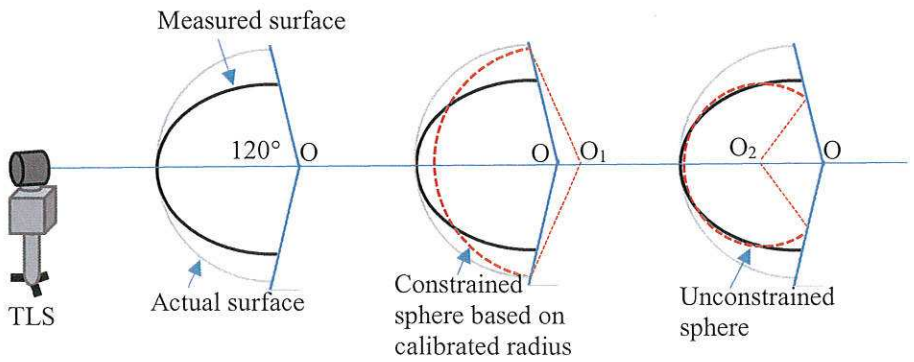

FIGURE 4. Error in the center coordinate because of apparent squishing of sphere

error in the center O_1O. It is difficult to quantify the center error O_1O because the true center O is an unknown quantity. However, the measured data does provide another potentially useful quantity, the unconstrained least-squares best-fit radius, from which we can estimate the error in the center O_1O through a simple simulation.

For this purpose, we first perform an unconstrained orthogonal least-squares fit on the measured data to determine the unconstrained radius r_{uc}. This provides an estimate of the extent of squishing or flaring of the sphere for this TLS/target combination under these measurement conditions. We then numerically generate a sphere data set with a radius r_{uc}, centered at a distance $r-r_{uc}$ from the origin where r is the calibrated radius of the sphere, and truncated over a cone opening angle of 120°. The data is generated at the same sampling interval as that of the measured data. We then perform a constrained orthogonal least-squares fit with a radius equal to the calibrated radius of the sphere target. The distance of the constrained center from the origin of the coordinate system is an estimate of the center error O_1O. In Fig. 5, we plot the center error as a function of the unconstrained radius for a sphere of nominal radius 50 mm. The plot shows that the error in locating the center increases by 0.24 mm for every 1 mm change in the observed unconstrained radius.

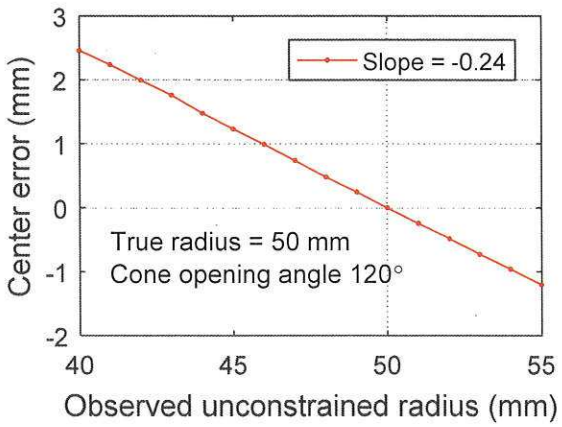

FIGURE 5. Center error along the TLS ranging direction as a function of unconstrained radius

The plot in Fig. 5 may be assumed to be linear for all practical purposes, although in reality it is not. The slope of the graph is -0.24 for a cone opening angle of 120°. The slope factor can be calculated for other cone opening angles in the same manner as described above. While Fig. 5 is based on a sphere of nominal radius 50 mm placed 10 m away and sampled at 92 ppd, simulations indicate that the results are not strongly influenced by the distance to the target, the point density, or the radius of the sphere.

Verifying the simulation through an experiment

In order to experimentally validate the above simulation, we mounted a sphere of nominal radius 50 mm on an aluminum plate as shown in Fig. 1(b). The front surface of the plate is media-blasted to a matte finish. The sphere-center to plate distance was calibrated on a contact probe CMM and determined to be 0.02 mm.

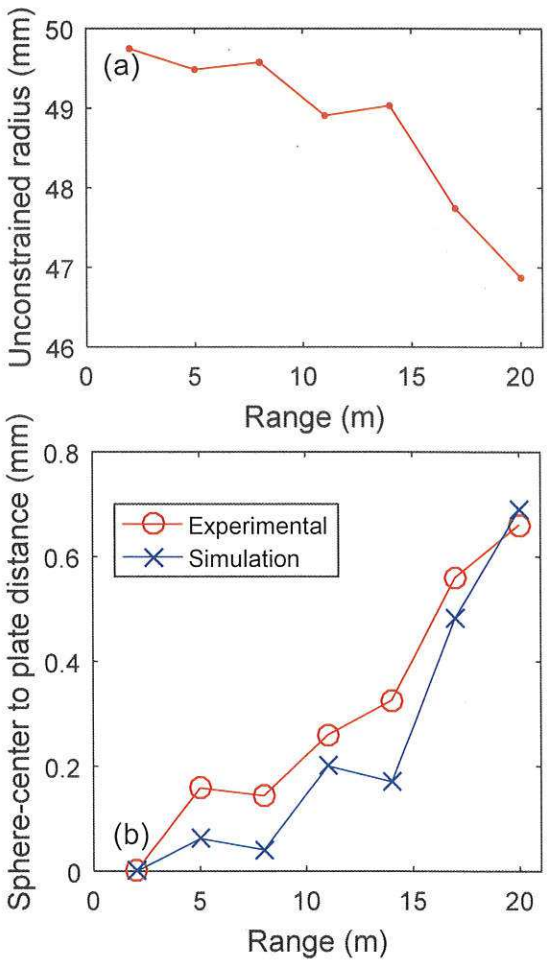

FIGURE 6. (a) Unconstrained radius as a function of distance (b) Sphere-center to plate distance

The artifact is scanned four times each at distances of 2 m through 20 m in increments of

3 m. The sphere data from the scan is fit to an unconstrained radius least-squares best-fit sphere and the resulting average radius from the four scans as a function of range is shown in Fig. 6 (a). It is clear that there is considerable squishing at the 20 m distance compared to the 2 m distance, with an unconstrained radius of 46.9 mm at 20 m and 49.7 mm at 2 m. From the simulations in the previous section, we anticipate the center to have moved by -0.24*(46.9-49.7) = 0.672 mm. The experimentally determined change of the sphere-center to plate distance is 0.66 mm, which is in excellent agreement with the simulations. Fig. 6(b) shows the change in the sphere-center to plate distance with respect to that at the reference position (2 m distance) obtained experimentally at the different ranges along with the simulation predictions based on unconstrained radius. This experiment validates the simulation and clearly confirms the movement of the constrained fit center because of sphere squishing/flaring.

CONCLUSIONS

TLSs are increasingly used in applications requiring accuracies on the order of a few tenths of a millimeter or more. However, the error sources in these systems are not carefully documented and detailed uncertainty budgets are not available. In this context, we describe the challenges associated with measuring a spherical geometry using a TLS. We have found that the sphere point cloud obtained from a TLS is impacted by the material in close vicinity to the sphere and this sometimes results in the sphere appearing squished or flared. Other factors such as averaging of the returns over a laser spot, the shape of the spot, etc., also affect squishing/flaring. While the error in the observed radius due to squishing/flaring can be easily quantified, the error in the center location is more challenging to estimate. For this purpose, we built the plate-sphere artifact, where the distance from the center of the sphere to the plate is calibrated. We infer the error in the sphere center location from the calculated distance between the sphere center and the plate. The experiments and simulations described in this paper indicates that care must be taken when processing TLS data because of the potential for error sources that are not yet understood.

Many applications require stitching of point clouds which in turn require registration. Based on the results in this study, obtaining sub-millimeter accuracy during registration using sphere targets will be a challenge. Also, this study clearly indicates that if relative range measurements are performed (i.e., measurements along the radial direction of a scanner) using sphere targets, the observed error may not only be due to the intrinsic error in the range measurement technology, but also due to the geometry of the sphere target and the properties of the surfaces that surround it.

REFERENCES

[1] Beraldin J.-A, Mackinnon D, and Cournoyer L, Metrological characterization of 3D imaging systems: progress report on standards developments, 17th International Congress of Metrology, 2015

[2] Lichti D D, Gordon S J, Stewart M P, Franke J, and Tsakiri M, Comparison of digital photogrammetry and laser scanning, Proceedings of International Workshop on Scanning for Cultural Heritage Recording - Complementing or Replacing Photogrammetry, Corfu, Greece, September 1-2.

[3] Rachakonda P, Muralikrishnan B, Lee V, Sawyer D, Phillips S and Palmateer J. A method of determining sphere center to center distance using laser trackers for evaluating laser scanners, Proceedings of the Annual Meeting of the ASPE, Boston, 2014.

[4] Bala Muralikrishnan, Meghan Shilling, Prem Rachakonda, Wei Ren, Vincent Lee, Daniel Sawyer, Toward the development of a documentary standard for derived-point to derived-point distance performance evaluation of spherical coordinate 3D imaging systems, Journal of Manufacturing Systems, 37, 2015, p. 550-557